

# A simulation analysis of backside-illuminated multi-collection-gate image sensor employing Monte Carlo method

Kazuhiro Shimonomura  
College of Science and Engineering  
Ritsumeikan University  
Kusatsu, Shiga 525-8577  
Email: skazu@fc.ritsumei.ac.jp

Vu Truong Son Dao      Takeharu G. Etoh  
Research Institute of Science and Technology      Ritsumeikan University  
Kusatsu, Shiga 525-8577

Yoshinari Kamakura  
Graduate School of Engineering  
Osaka University  
Suita, Osaka 565-0871

**Abstract**—Ultra-high speed image sensors have been developed and applied to various field of science and engineering. Toward the temporal resolution of 1ns, we have proposed a new structure of an image sensor, a backside-illuminated multi-collection-gate image sensor (BSI MCG image sensor). In order to evaluate the performance, it is necessary to simulate the paths of photoelectrons from the generation site to a collecting gate. The performance depends on several factors, including randomness in motion of the electrons which is considerable in the design of the sensor operating at the sub-nanosecond time scale. It is impossible to address this factor by using a device simulation based on the drift diffusion model. A Monte Carlo method is an effective tool to evaluate the effect of the randomness. In this paper, factors affecting the temporal resolution of the sensor are studied by using the Monte Carlo simulator.

## I. INTRODUCTION

An ultra-high speed image sensor with in-pixel storage has been developed and its application is expanding in various fields of advanced science and engineering. Since the pioneering work on a CCD image sensor of 1M frames per second [1], Etoh et al. have been updating the highest frame rate of the image sensor and the latest device achieved 16M frames per second (frame interval is 62.5ns) [2]. Toward the frame interval of 1ns, we have recently proposed a new structure of image sensor, a backside-illuminated multi-collection-gate image sensor (BSI MCG image sensor) [3], [4].

In order to evaluate the performance of the BSI MCG image sensor, it is necessary to simulate the paths of photoelectrons from the generation site to the collecting gate. This varies according to several factors [4], and randomness in motion of the electrons is considerable in this design of the sensor operating on the sub-nanosecond time scale. It is impossible to address this factor by using a device simulation based on the drift diffusion model, and Monte Carlo method can be an effective tool.

In this paper, the following issues are studied by using the Monte Carlo simulation: (1) The mean traveling time of photoelectrons from the generation site to the collecting gate and its standard deviation, (2) The rate of electrons which reach to the front side, (3) The rate of electrons arriving to the appropriate collecting gate (selective collection). In addition, (4) effect of the back side bias voltage and the wavelength of

the incident light to the traveling time is evaluated, followed by a discussion of a temporal resolution of the BSI MCG image sensor.

## II. STRUCTURE OF BSI MCG IMAGE SENSOR

In the BSI MCG image sensor, each pixel has multiple collection gates surrounding the center of the pixel, and a storage gate which accumulates a frame's signal electrons is attached to each collection gate [3].

In the simulation in this paper, we used the pixel design with six collection gates, reported in [4]. Here we describe the outline of the structure and operation of the design. Each pixel element on the front side shapes a distorted hexagon (Fig.1). Six collection gates (A1-A6) are around the pixel center, and a storage gate (B1-B6) is attached to each collection gate, which are surrounded by the exit and the transfer gates (C1-C6, D1-D6) to deliver the image signals to the outside of the sensor after capturing six consecutive image signal packets. The channel stop with a water-strider-like shape separates the collection gates in the pixel. The rhombus surrounded by the dashed line defines single pixel area. Signal electrons generated from incident photons within the square rhombus are guided by the p-well layer which prevents the signal electrons from migrating to the storage and transfer gates (Fig.2), and collected by one assigned collection gate, "the collecting gate" (A1 in Figs.1 and 2), to which a higher gate voltage is applied.

In the operation for image capturing, signal electrons generated on the backside travel toward the front side in accordance with the potential distribution (Fig.3) and are collected by the collecting gate. On the back side, a thin p+ layer is formed to eliminate the dark current by recombination with the holes filling the layer. Also a strong negative bias voltage ( $V_B$ ) is applied to the back side for generating the potential gradient which sends signal electrons toward the front side. The whole area except the channel stop forms a plane buried CCD channel, which is depleted before image capturing. The channel potential at the collecting gate is higher than those of other collection gates, but slightly lower than the channel potential of the storage gates. Electrons collected by the collecting gate are automatically drained to the storage gate and accumulated there. The channel at the collecting gate is always depleted, which keeps the very high travel speed of

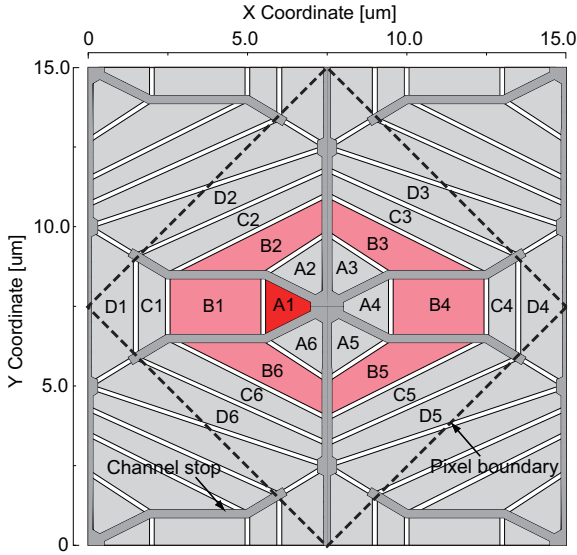


Fig. 1. Planer layout of a distorted hexagonal multi-collection-gate image sensor. Electrodes include collection gates (A1-A6), storage gates (B1-B6), exit gates (C1-C6), and transfer gates (D1-D6). Here, A1 is collecting gate, to which a higher gate voltage is applied. Dark gray shows channel stops.

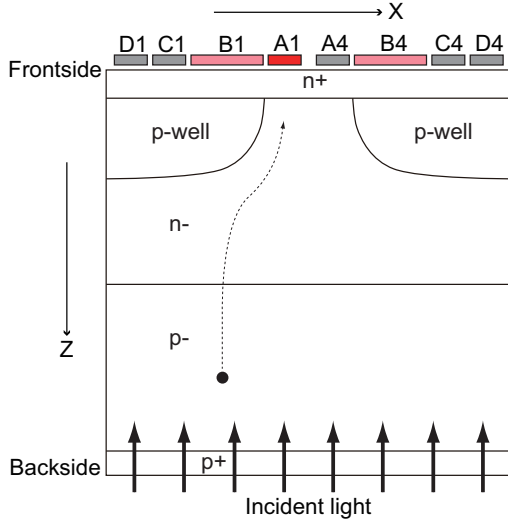


Fig. 2. Cross section of the multi-collection-gate image sensor. This is based on the structure of the tetratified BSI image sensor [2].

the signal electrons passing through the collecting gate. The speed suddenly lowers at the storage gate, since charges are accumulating there during the image capturing phase.

The collecting gate is switched by raising the gate voltage in turn, six consecutive frames can be captured in this design. The minimum temporal resolution of the BSI MCG image sensor theoretically depends on a distribution of the traveling time from the generation sites to the collecting gate of signal photoelectrons.

### III. MONTE CARLO SIMULATION

For analyzing the performance of the multi-collection-gate image sensor which operates on the sub-nanosecond time

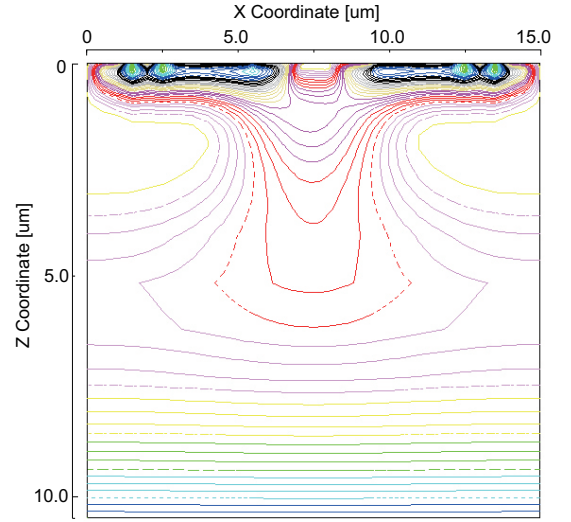


Fig. 3. Potential profile in the cross section at  $y=7.5\mu\text{m}$  of the multi-collection-gate image sensor. The figure shows the potential profile from the front side to  $10\mu\text{m}$ .

TABLE I. SIMULATION CONDITION.

Pixel size [ $\mu\text{m}$ ]	15.0 (diagonal), 10.6 (a side)
Thickness of the sensor [ $\mu\text{m}$ ]	33
Thickness of the backside Boron layer [nm]	1000
Wave length ( $\lambda$ ) [nm]	450, 500, 700
Absorption coefficient ( $\alpha$ ) [ $\text{cm}^{-1}$ ]	$2.00 \times 10^4$ , $1.11 \times 10^4$ , $0.219 \times 10^4$
Backside voltage ( $V_B$ ) [V]	-40, -42, -44

scale, randomness in motion of the electrons is considerable for estimating the temporal resolution of the sensor. In order to evaluate that, it is necessary to calculate the paths of individual photoelectrons by simulating their motion under the influence of applied electric field and scattering processes, i.e., phonon scatterings, scattering with ionized impurities, and impact ionization at high electric field. The Monte Carlo method can be an effective tool to address these factors. Here, we use the full band Monte Carlo simulation model which is the most accurate model [5] to analyze a photoelectron transport in the proposed image sensor. In the simulation, the potential distribution, which is calculated based on the design described in the previous section, is provided to the MC simulator as a reference table, and the 2-dimensional motion of photoelectrons is calculated.

The traveling time of photoelectrons from the generation sites to the collecting gate is evaluated for different generation sites, back side voltage, and wavelength of the incident light. The generation sites of the photoelectron in  $z$  direction ( $z_0$ ) is determined by a random number conforming to an exponent function with attenuation coefficient defined by  $1/\alpha$ , where  $\alpha$  is an absorption coefficient. Number of particle is 1000 for each simulation. The simulation condition used here is shown in Table.1.

### IV. RESULTS

Fig.4 shows examples of electron paths of randomly selected 20 samples generated at  $x_0=1.0\mu\text{m}$  and  $7.5\mu\text{m}$  for the left and right figures, respectively. Although each photoelectron generated near the back side shows random motion due

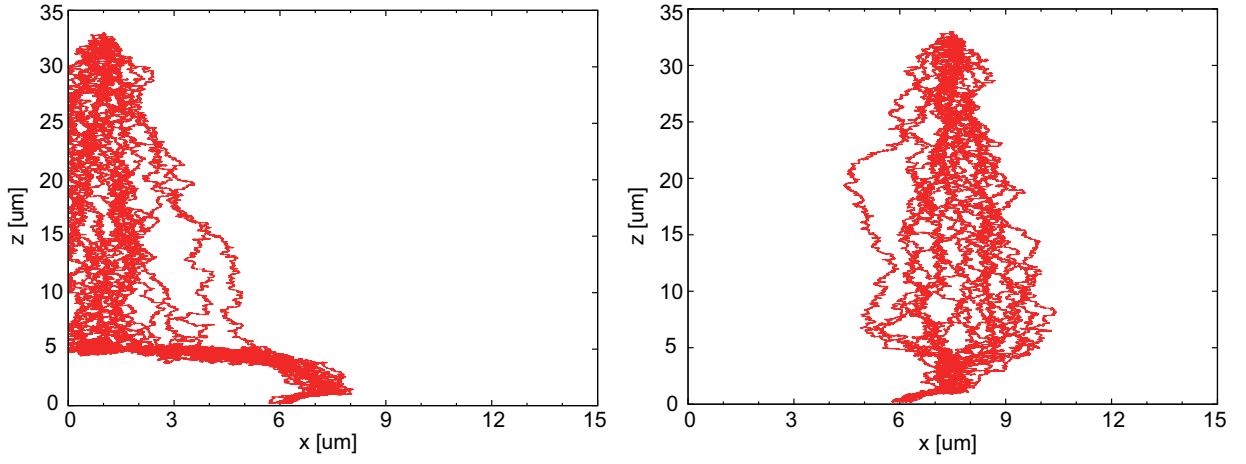


Fig. 4. Electron trajectories obtained from the Monte Carlo simulation.  $x$  coordinate of the generation sites of the electron is  $1.0\mu\text{m}$  (left) and  $7.5\mu\text{m}$  (right).  $V_B = -42\text{ V}$ ,  $\lambda = 500\text{ nm}$ .

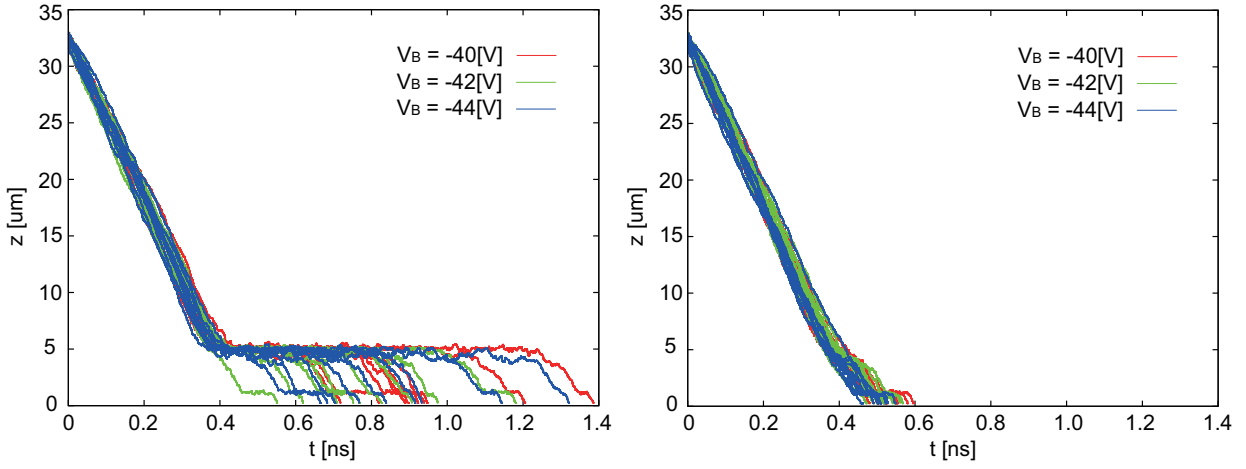


Fig. 5. Electron trajectories shown in the travel time vs.  $z$  coordinate.  $x$  coordinate of the generation sites of the electron is  $1.0\mu\text{m}$  (left) and  $7.5\mu\text{m}$  (right).  $V_B = -42\text{ V}$ ,  $\lambda = 500\text{ nm}$ .

to the phonon scatterings, it moves to the collecting gate on the front side in accordance with the potential gradient.

Fig.5 shows the time elapsing from a generation site to a certain depth. The variation of trajectories from the back side to around  $z = 5\mu\text{m}$  is not so large and is mainly caused by the difference of the penetration depth  $z_0$ . There is a large variation in the trajectories at around  $z = 5\mu\text{m}$  where the photoelectrons move in  $x$  direction. As the result, the travel time varied among the samples generated even at the same site. For the different back bias voltages, the difference of the trajectories is so significant.

Fig.6 shows the histogram of the travel time for different generation sites and different back side bias voltages. The variation of the traveling time limits the temporal resolution of the sensor, the mean and standard deviation  $\sigma$  of the traveling time was calculated. The mean travel times from  $x_0 = 1.0\mu\text{m}$ , near the pixel boundary, are  $0.84\text{ns}$  ( $\sigma = 0.228\text{ns}$ ),  $0.81\text{ns}$  ( $\sigma = 0.230\text{ns}$ ), and  $0.79\text{ns}$  ( $\sigma = 0.225\text{ns}$ ) for  $V_B = -40$ ,  $-42$ , and  $-44\text{ V}$ , respectively. The mean travel times from  $x_0 = 7.5\mu\text{m}$ , at the center of the pixel, are  $0.54\text{ns}$  ( $\sigma = 0.051\text{ns}$ ),

$0.52\text{ns}$  ( $\sigma = 0.048\text{ns}$ ), and  $0.51\text{ns}$  ( $\sigma = 0.044\text{ns}$ ) for  $V_B = -40$ ,  $-42$ , and  $-44\text{ V}$ , respectively.

Fig.7 shows the histogram of the travel time for different wavelength of the incident light. The mean travel times are  $0.623\text{ns}$  ( $\sigma = 0.164\text{ns}$ ),  $0.616\text{ns}$  ( $\sigma = 0.172\text{ns}$ ), and  $0.562\text{ns}$  ( $\sigma = 0.167\text{ns}$ ) for  $\lambda = 450\text{ nm}$  (blue),  $500\text{ nm}$  (green), and  $700\text{ nm}$  (red), respectively.

As discussed in [4], the temporal resolution is determined by the distribution of the traveling time. If we use the standard deviation  $\sigma$  as the index of the spread of the distribution, the simulation results above suggest that the differences of the back bias voltage and the wavelength have relatively little effect on the temporal resolution while the mean traveling time changes consistent with a predictable result. On the other hand, the difference of the planar generation sites ( $x_0$  in this simulation) substantially affects the temporal resolution as well as the mean traveling time. If the generation sites are limited around the center of the pixel in some way and the temporal resolution is defined as  $2\sigma$ , it can be reduced to about  $100\text{ ps}$ .

To evaluate the overall performance in this design, paths

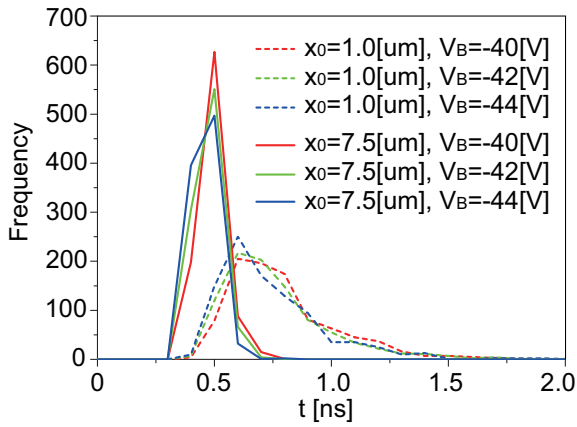


Fig. 6. Histogram of the travel time for different generation sites ( $x_0 = 1.0\ \mu\text{m}$  and  $7.5\ \mu\text{m}$ ), and back side bias voltages ( $V_B = -40, -42,$  and  $-44\ \text{V}$ ).

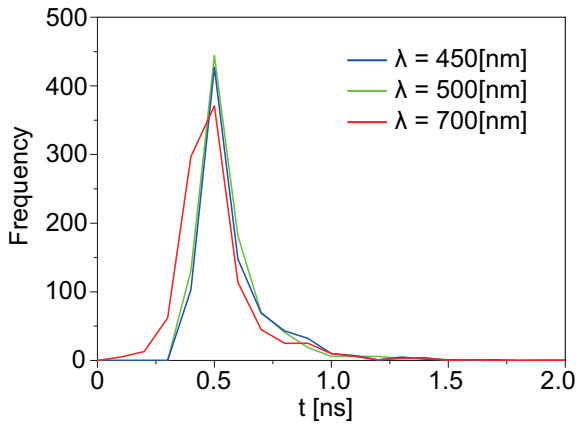


Fig. 7. Histogram of the travel time for different wavelength of the incident light ( $\lambda = 450, 500,$  and  $700\ \text{nm}$ ).  $V_B = -42\ \text{V}$ ,  $x_0$  is determined by a random number between  $1\ \mu\text{m}$  to  $14\ \mu\text{m}$ .

of 1200 electrons which were randomly generated between  $x_0 = 1\ \mu\text{m}$  to  $14\ \mu\text{m}$  were simulated. The mean traveling time of photoelectrons and its standard deviation were 0.621 ns and 0.170 ns, respectively. 69.3% of the generated electrons reached to the collection gates on the front side, and other electrons disappear in the backside hole accumulation layer due to the recombination. A few electrons were collected by a different collection gate and the success rate of selective collection was 99.2% in this simulation.

## V. CONCLUSION

In this paper, the temporal resolution of the sensor were evaluated by using the Monte Carlo simulator. The results are summarized as follows: (1) The mean traveling time and standard deviation were 0.621 ns and 0.170 ns, respectively. (2) 69.3% of the generated electrons reached to the collection gates on the front side. (3) 99.2% of the electrons could be collected by the collecting gate. These show that the temporal resolution of less than 1ns is realizable by the current design even considering randomness in motion of the signal electrons. In addition, (4) the most dominant factor affecting to the temporal resolution was the planar generation sites rather than the back side bias voltage and wavelength of the incident light.

This suggests that the temporal resolution can be reduced by additional optics such as on-chip micro lens which guides the incident light to the pixel center as well as more appropriate design of the doping concentration distribution of p-well layer.

## REFERENCES

- [1] T. G. Etoh, D. Poggemann, A. Ruckelshausen, A. Theuwissen, G. Kreider, H.-O. Folkerts, H. Mutoh, Y. Kondo, H. Maruno, K. Takubo, H. Soya, K. Takehara, T. Okinaka, Y. Takano, T. Reisinger, C. Lohmann, "A CCD image sensor of 1 Mframes/s for continuous image capturing of 103 frames," Digest of Technical Papers, ISSCC2002, pp.46-47, 2002.
- [2] T. G. Etoh, D. H. Nguyen, S. V. T. Dao, C. L. Vo, M. Tanaka, K. Takehara, T. Okinaka, H. v. Kuijk, W. Klaassens, J. Bosiers, M. Lesser, D. Ouellette, H. Maruyama, T. Hayashida, T. Arai, "A 16 Mfps 165 kpixel backside-illuminated CCD," Digest of Technical Papers, ISSCC2011, pp.406-407, 2011.
- [3] T. G. Etoh, V. T. S. Dao, T. Yamada, and E. Charbon, "Toward One Giga Frames per Second Evolution of In-situ Storage Image Sensors," Sensors, vol. 13, no. 4, pp.4640-4658, 2013.
- [4] V. T. S. Dao, K. Shimonomura, Y. Kamakura, and T. G. Etoh, "Simulation analysis of a backside-illuminated multi-collection-gate image sensor," ITE Trans. on Media Technology and Applications, vol. 2, no. 2, pp.144-122, 2014.
- [5] T. Kunikiyo, M. Takenaka, Y. Kamakura, M. Yamaji, H. Mizuno, K. Taniguchi, and C. Hamaguchi, "A Monte Carlo simulation of anisotropic electron transport in silicon including full band structure and anisotropic impact ionization model," J. Appl. Phys., vol. 75, no. 1, pp. 297-312, 1994.